

GEOMETRICAL SIMILARITY IN SATURATED POOL BOILING

J. S. TURTON

Department of Engineering, University of Aberdeen

(Received 10 August 1964 and in revised form 1 June 1965)

Abstract—The concept of the geometrical similarity of a random distribution of spherical bubbles attached to the boiling surface is introduced and the mechanism of bubble removal from a horizontal flat surface in saturated nucleate pool boiling is discussed. The concept of geometrical similarity is applied to the regime of interacting bubbles in nucleate pool boiling and this leads to an expression for heat transfer through a quiescent sub-layer which is assumed to exist in the fluid immediately adjacent to the boiling surface.

The heat flux due to nucleate pool boiling is related to the rate of vapour production at the boiling surface. The regime of coalescing bubbles in nucleate pool boiling is studied from the basis of geometrical similarity of the phase boundaries. The critical heat flux is assumed to occur at a particular phase front geometry. This leads to the following correlation for the critical heat flux in saturated pool boiling for clean, smooth wetted surfaces:

$$\dot{q}_{BO} = 1.25 \{g \Delta T_0 K_L L^2 \rho_V (\rho_L - \rho_V)\}^{0.333} \text{ in Btu, ft, h units.}$$

This expression shows satisfactory correlation of critical heat flux data for a wide range of liquids.

NOMENCLATURE

A ,	area of phase front, l^2 ;	l ,	length, l ;
a ,	bubble growth factor, $lt^{-0.5}$;	l_M ,	mean attached vapour volume per unit area of boiling surface, l ;
B ,	buoyancy force on a bubble, mlt^{-2} ;	m ,	mass, m ;
C_F ,	coefficient of resistance to bubble motion;	N_D ,	dimensionless bubble departure density;
C_{FD} ,	coefficient of resistance to bubble motion at bubble departure;	N_E ,	evaporation number, $N_E = \rho_L c_L T / \rho_V L$;
C_H ,	coefficient of latent heat transport;	N_G ,	dimensionless bubble population density;
C_I ,	mixing coefficient;	N_T ,	superheat number, $N_T = \Delta T / T$;
c ,	specific heat at constant pressure, $l^2 t^{-2} T^{-1}$;	n_M ,	mean number of attached bubbles per unit area of boiling surface, l^{-2} ;
D ,	bubble diameter, l ;	P ,	absolute pressure, $ml^{-1} t^{-2}$;
\dot{E} ,	evaporation rate from liquid to vapour, $ml^{-2} t^{-1}$;	Pr ,	Prandtl number;
F ,	component normal to boiling surface of fluid resistance to bubble motion, mlt^{-2} ;	\dot{q} ,	rate of heat transfer per unit area of surface, mt^{-3} ;
f ,	bubble frequency, t^{-1} ;	R ,	bubble radius, l ;
g ,	acceleration due to gravity, lt^{-2} ;	Re ,	Reynolds number;
h ,	heat-transfer coefficient, $h = \dot{q} / \Delta T$, $mt^{-3} T^{-1}$;	r ,	radial co-ordinate for spherical bubble, l ;
\dot{I}_M ,	mean bubble initiation rate per unit area of boiling surface, $l^{-2} t^{-1}$;	r_S ,	radius of vapour-solid contact circle, l ;
K_L ,	liquid thermal conductivity, $mlt^{-3} T$;	S ,	component normal to boiling surface of surface tension force acting on bubble, $ml^{-1} t^{-2}$;
$k_1, 2, 3$,	factors introduced in text;	T ,	temperature, T ;
L ,	latent heat of vaporization, $l^2 t^{-2}$;	ΔT ,	temperature difference between sur-

	face and saturation temperature of fluid, T ;
t ,	time, t ;
t_D ,	duration of bubble contact with boiling surface, t ;
U ,	velocity normal to boiling surface, lt^{-1} ;
V ,	volume, l^3 ;
V_D ,	volume of bubble at departure from surface, l^3 ;
x ,	co-ordinate normal to boiling surface, l ;
α ,	thermal diffusivity, $\alpha = K/\rho c$, l^2t^{-1} ;
β ,	contact angle;
μ ,	coefficient of viscosity;
ρ ,	density, ml^{-3} ;
σ ,	surface tension, mt^{-2} ;
ϕ ,	factor defined in appendix.

Subscripts

B ,	due to boiling;
D ,	at bubble departure;
F ,	due to fluid resistance to motion;
H ,	due to transport of latent heat of vaporization;
I ,	due to convective mixing;
L ,	liquid;
M ,	mean value;
O ,	value at the critical heat flux;
S ,	solid surface;
V ,	vapour.

INTRODUCTION

STUDIES of the fluid dynamics associated with the motion of bubbles in nucleate pool boiling have provided the basic concepts of several theories. Chang and Snyder [1] developed the concept of a thermal diffusivity for the agitated liquid close to the boiling surface. Tien [2] proposed a hydrodynamic model based on the flow of liquid near a nucleating site which emits a stream of bubbles. Two flow regimes were discussed, namely, one of discontinuous bubble emission at low heat-transfer rates and one of high nucleating site density where mutual influence between bubbles is significant. Zuber [3] also distinguishes a regime of isolated bubbles in low heat flux nucleate boiling from one of bubble interference at higher heat fluxes and derives expressions which relate heat flux, bubble departure diameter and nucleating site density for

the regime of isolated bubbles. In addition, equations predicting values at transition from isolated bubbles to bubble interference are derived.

If the mechanism of bubble growth and departure is one of thermal and mechanical interaction between bubbles it does not seem possible to use the geometry of a single bubble as a basis for theoretical consideration of the boiling problem. In this paper the geometry of a complete distribution of bubbles attached to the boiling surface and departing from it forms the basis of the theory. A dimensionless bubble population density is proposed and requirements for the geometrical similarity of a random distribution of attached bubbles are given. This geometrical concept is extended into the region of coalescing bubbles and leads to a correlation for critical heat flux data.

The problem of the critical heat flux has been studied by several authors. Addoms [4], Borishankysy [5] and Kutateladze [6] investigated the dynamics of the boiling process and employed dimensional analysis to obtain expressions for the critical heat flux. Noyes [7] modified the expression obtained by Addoms in the light of experimental data for the saturated pool boiling of sodium. Deissler [8], Rohsenow and Griffith [10] and Chang and Snyder [1] proposed theories based on bubble dynamics. Zuber [11] considered the Taylor instability of a liquid vapour interface. A review of theories of critical heat flux for saturated pool boiling is given by Ivey [12].

The argument concerning critical heat flux in this paper is based on the premise that the critical condition exists at a particular geometrical configuration of the phase front. For this purpose a hypothetical phase front geometry is proposed which consists of portions of overlapping spheres. The similarity of the phase front geometry at the critical condition forms the basis of the critical heat flux correlation.

GEOMETRICAL SIMILARITY IN POOL BOILING

A geometrical model of nucleate pool boiling is now proposed. It is assumed that spherical vapour bubbles are produced from a random distribution of nucleating sites in a flat horizontal

boiling surface and grow within the superheated liquid lying above the surface. At any instant the attached bubbles present a random distribution of spheres of various sizes. If n_M is the mean number of bubbles attached to a unit area of surface and the mean total volume of attached vapour is l_M , a dimensionless bubble population density can be written:

$$N_G = n_M l_M^2 \quad (1)$$

The requirement for geometrical similarity of two distributions of attached bubbles, within the confines of their random nature are:

- (i) N_G has the same value;
- (ii) The bubble growth function,

$$\frac{R}{R_D} = f\left(\frac{t}{t_D}\right)$$

has the same form.

The bubble growth function determines the distribution of bubble sizes attached to any sufficiently large sample of boiling surface.

The quantity l_M is evaluated in the appendix for non-coalescing spherical bubbles:

$$l_M = \phi n_M R_D^3 \quad (2)$$

where ϕ is a factor which depends on the bubble growth function, hence

$$N_G = \phi^2 n_M^3 R_D^6 \quad (3)$$

The requirement for geometrical similarity of a stream of bubbles leaving a nucleating site may be obtained from a study of the geometry of two consecutive bubbles issuing from the same site. The centre to centre distance between consecutive bubbles is (U/f) where U is the mean velocity in the x direction of the bubbles over the centre to centre distance. Two streams of mature (no longer growing) bubbles are geometrically similar if the dimensionless group

$$N_D = \frac{U}{f R_D} \quad (4)$$

is the same for both streams.

Obviously, at certain values of N_G and N_D coalescence of the bubbles will occur. The degree of coalescence depends on the values of N_G and N_D , that is, on the geometrical configuration of

the attached and departing bubbles. The above geometrical concepts based on isolated spheres can be extended into the region of coalescences by regarding these as made up of overlapping spheres. Equations (2) and (3) can then be used to describe the phase front geometry in the regime of bubble coalescence and equation (4) can be extended to describe vapour columns, regarding these as made up of a succession of coalescent bubbles.

FORCES ON AN ATTACHED BUBBLE

The departure of attached bubbles from a horizontal surface was analysed by Fritz [13] on a basis of static equilibrium of buoyancy and surface tension forces. This gives the well-known expression for the departure diameter:

$$D_D = \text{const. } \beta \left\{ \frac{2\sigma}{g(\rho_L - \rho_V)} \right\}^{0.500} \quad (5)$$

where β is the contact angle at the base of the bubble.

Experimental observations of bubble departure diameter were made by Semeria [14] for a range of pressures and indicate considerably smaller diameters at high pressures than would be predicted by equation (5). Semeria gives the following correlation with pressure, P in atmospheres:

$$D_D = 1.6 P^{-0.5} \quad 2 < P < 20 \text{ atm abs}$$

This is clearly not in accord with equation (5). The following is a re-examination of the forces on an attached bubble in nucleate pool boiling.

Figure 1 shows a spherical vapour bubble of radius R during growth within a temperature boundary layer in liquid above a horizontal flat surface in saturated pool boiling. It is assumed that the surface is free of contaminants which inhibit wetting. The influence of surface tension on bubble growth is neglected. At any instant, r is a radial co-ordinate and \dot{E}_M is a mean evaporation rate into the bubble per unit area of phase boundary. The total evaporation rate into a bubble having a phase front area of A is:

$$\dot{E}_M A = k_1 A f \left(\frac{\partial T}{\partial r} \right)_M = A \dot{R} \rho_V \quad (6)$$

where $(\partial T / \partial r)_M$ is a mean radial temperature gradient for the whole bubble. It is now assumed

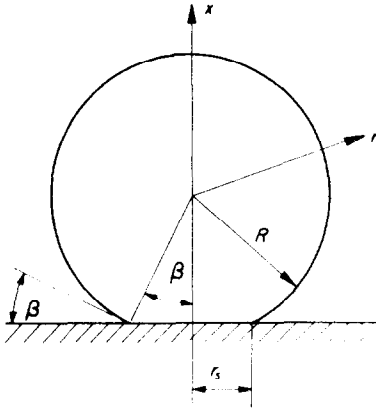


FIG. 1. Bubble geometry.

that the liquid velocity is zero immediately adjacent to the solid surface and that the growth of a circle of contact of vapour and solid is due only to the evaporation of the liquid molecules which lie immediately adjacent to the surface and which, for this purpose, can be considered to form a molecular monolayer next to the solid surface. It is further assumed that the evaporation of this layer is due to heat transfer from the solid surface and that the forces on this monolayer due to neighbouring molecules in the solid, liquid and vapour phases are such that the contact angle, β has negligible influence on its evaporation. Therefore, the evaporation rate per unit area of phase front taken for this condition at the solid surface, \dot{E}_S may be expressed in the form:

$$\dot{E}_S = k_{1S} f \left(\frac{\partial T}{\partial r} \right)_S = \dot{r}_S \rho_L \quad (7)$$

Equations (6) and (7) refer to instantaneous conditions and lead to the following relationship:

$$\frac{r_S}{R} = k_2 \frac{\rho_V}{\rho_L} \quad (8)$$

where k_2 is a factor which is governed by the temperature distribution surrounding the bubble throughout its history of growth. Since it depends essentially on the ratio of surface to mean evaporation rates at the phase front, k_2 is probably greater than unity.

If the buoyancy and surface tension forces are investigated for a bubble which is assumed spherical throughout its growth the resultant surface tension force in the x direction is:

$$\begin{aligned} S &= -2\pi r_S \sigma \sin \beta \\ &= \frac{-2\pi r_S^2 \sigma}{R} \end{aligned} \quad (9)$$

The buoyancy force in the x direction is:

$$B = \frac{4\pi}{3} R^3 (\rho_L - \rho_V) g \quad (10)$$

The ratio of surface tension force to buoyancy force at bubble departure from equations (8), (9) and (10) is:

$$\frac{S}{B} = \frac{-3k_2^2 \rho_V^2 \sigma}{2R_D^2 \rho_L^2 (\rho_L - \rho_V) g} \quad (11)$$

Figure 2 shows the ratio, $-S/Bk_2^2$ plotted for water over a range of pressures and computed from equation (11) with values of the bubble departure radius, R_D obtained from the experimental correlation given by Semeria [14]. It can be seen from the values in Fig. 2 that if equation (9) holds good the surface tension force is small by comparison with the buoyancy force for saturated pool boiling of water over a fairly wide range of pressures. Equation (9) suggests that bubble contact angles are smaller than those indicated by experimental measurements from visual methods [9], [15]. However, accurate visual observation of bubble contact angles may be difficult owing to refraction effects brought about by temperature gradients in the superheated liquid surrounding the bubble.

In the following theory the influence of surface tension on the bubble departure mechanism is neglected. It is assumed that, in low heat flux nucleate boiling, viscous and momentum forces associated with the dynamics of bubble growth are important factors in the mechanism of bubble departure.

Semeria [14] and Gaertner and Westwater [16] report experimental observations which indicate that at high heat fluxes in nucleate boiling the bubbles are prematurely removed from the surface by the intense agitation induced by neighbouring bubbles. Following Zuber [3] two regimes of nucleate boiling may be distinguished:

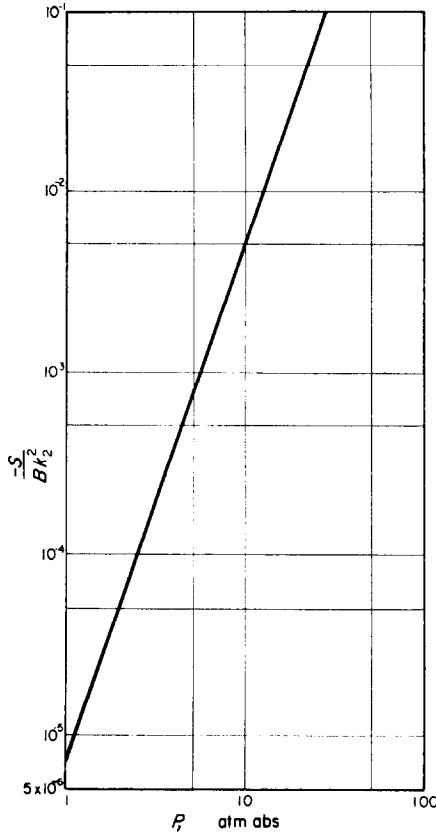


FIG. 2. Relationship between surface tension and buoyancy forces at bubble departure.

- (i) A regime of isolated bubbles where the dynamical interaction between neighbouring bubbles is negligible.
- (ii) A regime of interacting bubbles with a high degree of liquid turbulence.

The mechanism of bubble growth and departure is now discussed for each regime in turn.

REGIME OF ISOLATED BUBBLES

The growth of an isolated spherical bubble within a superheated liquid layer above a plane horizontal nucleating surface is now considered. The vertical component of the resistance, F on the bubble due to momentum and viscous forces during bubble growth is expressed in terms of the vapour density, ρ_V , a typical length dimension, R , and the mean radial liquid velocity at

the phase front, $\dot{R}(1 - [\rho_V/\rho_L])$. Hence on dimensional grounds:

$$F = - \frac{\rho_V}{2} \dot{R}^2 R^2 \left(1 - \frac{\rho_V}{\rho_L}\right)^2 \cdot C_F$$

where C_F is a coefficient of resistance. Introducing a condition for bubble departure:

$$B + F = 0$$

the following bubble radius at departure is obtained:

$$R_D = \frac{3\rho_V}{8\pi\rho_L} \left(1 - \frac{\rho_V}{\rho_L}\right) \frac{\dot{R}_D^2}{g} \cdot C_{FD} \quad (12)$$

Scriven [17] gives analytical solutions for spherical bubble growth in an infinite, uniformly superheated, non-turbulent liquid and deduces a bubble growth function of the form:

$$R = at^{0.500} \quad (13)$$

where $a = \text{const. } \alpha^{0.500}(N_E N_T)^n$,

$$0.500 \leq n \leq 1.000$$

for the condition

$$\left| \frac{c_L - c_V}{L} \right| \ll 1$$

From equations (12) and (13)

$$R_D = \text{const. } a^{1.333}$$

$$\left\{ \frac{\rho_V/\rho_L (1 - \rho_V/\rho_L) C_{FD}}{g} \right\}^{0.333} \quad (14)$$

The form of C_{FD} is not clear. Since the influence of neighbouring bubbles in the isolated bubble regime is assumed negligible it follows that C_{FD} is independent of bubble population density, i.e. independent of N_G . However, C_{FD} may be a function of a bubble growth Reynolds number which, for convenience, is here based on liquid properties:

$$Re_{LD} = R_D \dot{R}_D \left(1 - \frac{\rho_V}{\rho_L}\right) \frac{\rho_L}{\mu_L}$$

In addition, the ratio of vapour to liquid properties, such as

$$\frac{\rho_V}{\rho_L}, \frac{\mu_V}{\mu_L}$$

and corresponding Prandtl numbers, may influence C_{FD} .

The value of the bubble growth factor, a , may correspond to a cavity superheat at nucleation, ΔT_C rather than the mean surface superheat. The results of Gaertner and Westwater [16] tend to support this view since no conclusive variation in the bubble departure radius, R_D is indicated in the isolated bubble regime.

REGIME OF INTERACTING BUBBLES

The results of Gaertner and Westwater [16] show that for the region of interacting bubbles there is a pronounced reduction of bubble departure diameter with increase of heat-transfer rate. Equation (14) is, therefore, not applicable to this region. It is probable that, due to increase of liquid turbulence, there is a progressive thinning of the temperature boundary layer with increase of heat-transfer rate and that bubbles cease to grow when they extend sufficiently beyond this layer or push it away from the boiling surface and disperse the superheated liquid into the turbulent bulk. The bubbles are then removed from the boiling surface by the intense agitation set up by neighbouring bubbles. However, in the region of interacting bubbles with highly turbulent liquid it can still be suggested that there is a layer of quiescent liquid immediately adjacent to the boiling surface which can be regarded as a laminar sub-layer. It can be suggested that the thickness of this sub-layer is closely related to the bubble departure diameter, R_D . Since the bubbles are removed by the intense agitation set up by neighbouring bubbles, R_D therefore depends on bubble population density, i.e. on N_G . The highly turbulent nature of the flow suggests that Reynolds number effects may not be very important.

For conduction through the laminar sub-layer it is possible to form the equation:

$$\dot{q}_B = \frac{K_L \Delta T}{R_D} \cdot f(N_G, Re, Pr) \quad (15)$$

If Reynolds and Prandtl number influences are neglected it is possible to formulate expressions based on equations (3) and (15) which are compatible with the results of Gaertner and Westwater [16] for water at one atmosphere. The data

of reference 16 suggest a relationship between bubble departure radius and heat-transfer coefficient for the region of interacting bubbles which may be obtained by correlating the upper points of Fig. 3:

$$h = \frac{\dot{q}_B}{\Delta T} = 2 \times 10^2 K_L R_D^{-0.56} \quad (16)$$

in Btu, h, ft and degF units with $K_L = 0.40$ Btu/h ft degF.

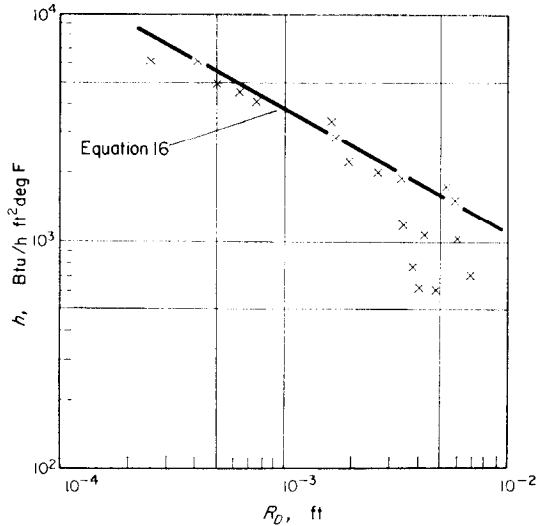


FIG. 3. Variation of heat-transfer coefficient with bubble departure radius in nucleate boiling of water at 1 atm. Comparison with experimental data of Gaertner and Westwater [16].

Reference 16 presents measurements of nucleating site density whilst the present theory is formulated in terms of a mean bubble population density. However, it is thought that although the mean bubble population density is considerably lower than the nucleating site density at low nucleate boiling heat fluxes, the two are almost equal at high heat fluxes since the liquid solid contact at the nucleating site is of very brief duration. An approximate relationship between bubble departure radius and the mean bubble population density can, therefore, be suggested from the data of reference 16 (see Fig. 4):

$$R_D = 7.17 \times 10^{-2} n_M^{-0.45} \quad (17)$$

in ft units.

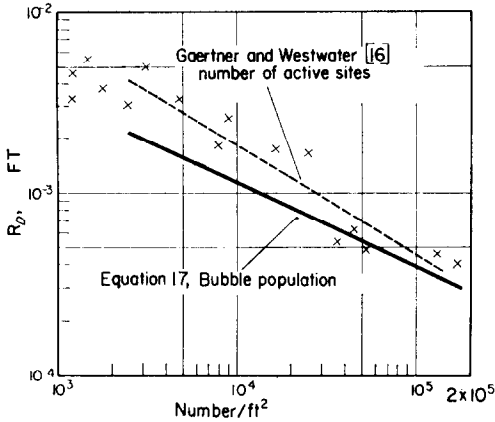


FIG. 4. Relationship between bubble population density and bubble departure radius in nucleate boiling of water at 1 atm. Comparison with experimental data of Goertner and Westwater [16].

Equations (16) and (17) yield an alternative correlation for the heat-transfer coefficient:

$$h = 8.75 \times 10^2 K_L N_M^{0.25} \quad (18)$$

Equation (18) is plotted for comparison with the relevant data from reference 16 in Fig. 5.

Equations (16) and (17) yield a relationship of the form of equation (15). Using equation (3) and neglecting Reynolds and Prandtl number influences:

$$\dot{q}_B = \frac{K_L \Delta T}{R_D} \times 1.675 \times 10^{-3} \times \phi^{1.333} N_G^{-0.667} \quad (19)$$

Thus the results of reference 16 appear compatible with the theory of geometrical similarity

and the concept of conduction through a laminar sub-layer in the regime of interacting bubbles.

HEAT-TRANSFER RATE

Three mechanisms of heat transfer may be distinguished in the nucleate boiling regime:

- (i) Natural convection in the liquid
- (ii) Transport of latent heat due to removal of bubbles from the surface
- (iii) Convective mixing due to bubble motion.

Merte and Clark [18] and Graham and Hendricks [19] point out that the natural convection mechanism is enhanced under conditions of increased acceleration with consequent suppression of nucleate boiling at low heat fluxes. Also, these authors present experimental evidence which suggests that the natural convection mechanism is active well into the nucleate boiling regime. However, at gravitational acceleration the heat-transfer rate due to natural convection appears to be comparatively small in the nucleate boiling of a saturated pool. Forster and Greif [20] discuss convective mixing of the liquid and propose a vapour liquid interchange mechanism. In this, a quantity of superheated liquid surrounding each bubble is pushed away from the surface into the cooler bulk as a result of bubble growth.

In the following analysis it is assumed that each bubble transports during growth and departure a liquid volume proportional to the volume of the departing bubble from some mean temperature, T_M to a region of saturation

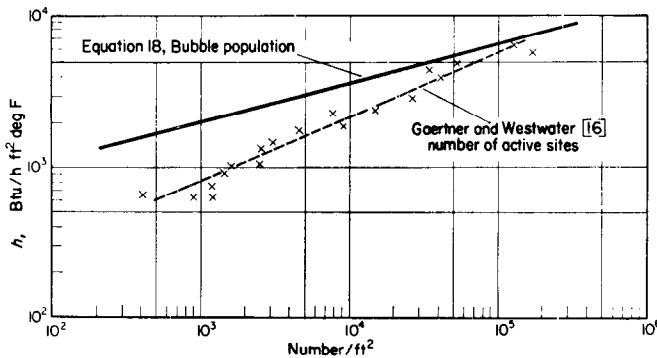


FIG. 5. Variation of heat-transfer coefficient with bubble population density in nucleate boiling of water at 1 atm. Comparison with experimental data of Goertner and Westwater [16].

temperature, T . The rate of latent heat transport per unit area due to departing bubbles without coalescence is:

$$\dot{q}_H = \dot{I}_M V_D \rho_V L$$

The total heat flux from the surface, including liquid transport away from the surface is:

$$\dot{q}_1 = \dot{I}_M V_D \{ \rho_V (c_L T + L) + k_3 \rho_L c_L T_M \}$$

where k_3 is a constant. The mass convected by this process must be balanced by a migration of liquid towards the surface, consequently the heat flux to the surface is:

$$\dot{q}_2 = \dot{I}_M V_D (\rho_V + k_3 \rho_L) c_L T$$

The net heat flux from the surface due to the combined processes of latent heat transport and convective mixing is:

$$\dot{q}_B = \dot{q}_1 - \dot{q}_2 = \dot{I}_M V_D \{ \rho_V L + k_4 \rho_L c_L (T_M - T) \}$$

which may be written:

$$\dot{q}_B = \dot{I}_M V_D \rho_V L \{ 1 + C_I N_E N_T \} \quad (20)$$

The ratio of the heat transfer due to convective mixing to that due to latent heat transport is $C_I N_E N_T$ where C_I is a mixing coefficient and N_E and N_T are the evaporation and superheat numbers respectively as defined in the nomenclature. The value of C_I may be estimated by experimental observations of heat-transfer rate and bubble departure rate and diameter. Forster and Greif [20] supported by data given for subcooled boiling by Gunther and Krieth [21], deduce that for water at atmospheric pressure the latent heat transport mechanism accounts for only a small fraction of the heat transfer in nucleate boiling. The value of N_E for water is plotted in Fig. 6 for a range of pressures. This suggests that although convective mixing may be the dominant mechanism at atmospheric pressure, the contribution to the total heat transfer of this mechanism becomes progressively smaller as the pressure increases. It is probably negligible at high pressures.

Equation (20) is strictly applicable only to the isolated bubble regime, but it can be modified to take account of bubble coalescence:

$$\dot{q}_B = \dot{I}_M V_D \rho_V L (C_H + C_I N_E N_T) \quad (21)$$

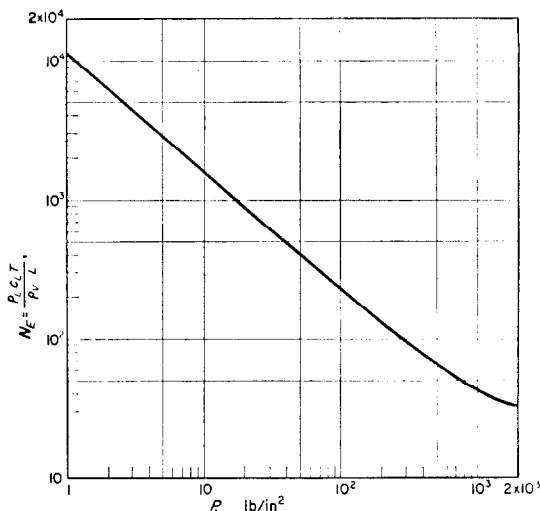


FIG. 6. Variation of evaporation number, N_E with pressure for water.

where the coefficients C_H and C_I are functions of the phase front geometry, i.e. functions of N_G and N_D .

CRITICAL HEAT FLUX

For nucleate boiling near to the critical heat flux the approximation, $f = 1/t_D$ can be made. Equation (21) then becomes, using equations (3) and (4):

$$\dot{q}_B = \frac{4\pi U N_G^{0.333}}{3\phi^{0.667} N_D} \cdot \rho_V L (C_H + C_I N_E N_T) \quad (22)$$

since

$$n_M = \dot{I}_M t_D$$

Now, if U is regarded as being equal to the velocity of a bubble swarm rising within a liquid, the equation of buoyancy and resistance forces on each bubble yields:

$$U^2 = \frac{8g}{3C_F} \cdot \frac{\rho_L - \rho_V}{\rho_V} \cdot R_D, \quad C_F = f \left(\frac{\rho_V}{\rho_L}, N_D, Re, Pr \right) \quad (23)$$

where R_D is taken as a representative bubble length and ρ_V as a representative fluid density.

If the coefficient of resistance to bubble motion, C_F is assumed constant and the natural

convection heat-transfer component is negligible, substitution for R_D from equation (15) in equation (23) gives, neglecting Reynolds and Prandtl number influences:

$$U = \left\{ \frac{gK_L \Delta T (\rho_L - \rho_V)}{\dot{q}_B \rho_V} \right\}^{0.500} \times f(N_G) \quad (24)$$

and the heat flux for conditions approaching the critical can be written, from equations (22) and (24):

$$\dot{q}_B = f(N_G, N_D) \cdot \{\rho_V L^2 g K_L \Delta T (\rho_L - \rho_V)\}^{0.333} (C_H + C_I N_E N_T)^{0.667} \quad (25)$$

Here the influence of ϕ , a factor depending on the bubble growth function, is neglected.

It is now possible to argue from the premise that the critical heat flux occurs at a particular geometrical configuration of the phase fronts, i.e. at particular values of N_G and N_D . If N_G and N_D are uniquely related the value of $f(N_G, N_D)$ in equation (25) is a constant at the critical condition and it is possible to write an expression for the critical heat flux:

$$\dot{q}_{BO} = \text{const.} \{g \Delta T_0 K_L L^2 \rho_V (\rho_L - \rho_V)\}^{0.333} (C_H + C_I N_E N_T)^{0.667} \quad (26)$$

Table 1 gives details of experimental measurements of the critical heat flux made by several experimenters for a selection of pure liquids boiling from smooth wetted surfaces. Figure 7 shows that reasonable correlation of this data (with the exception of some high pressure results) is obtained by the expression:

$$\dot{q}_{BO} = 1.25 \{g \Delta T_0 K_L L^2 \rho_V (\rho_L - \rho_V)\}^{0.333} \quad (27)$$

Although the last term in equation (26) is omitted from equation (27) a satisfactory correlation is still obtained. This suggests that heat transfer by convective mixing is negligible at the critical heat flux even at the lower pressures recorded in the data (See Table 1). The probable heat transfer mechanism is from wall to liquid across the quiescent laminar layer and thence by evaporation and latent heat transport to the bulk liquid.

Values of the critical heat flux given in Table 1

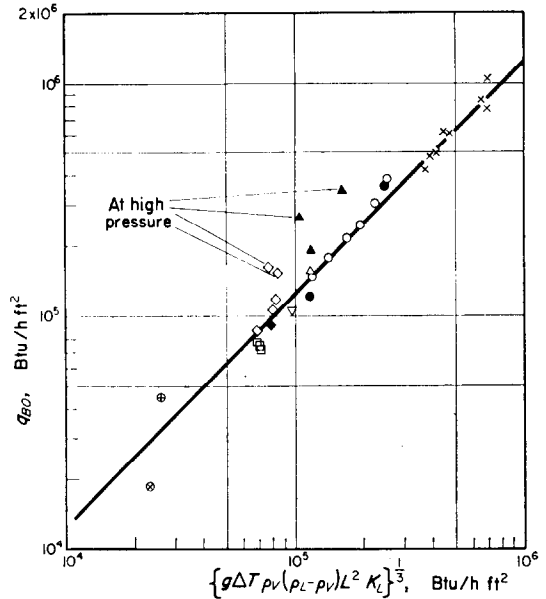


FIG. 7. Correlation of critical heat flux data contained in Table 1. Principal sources of fluid property data: references 24, 29 and 33-37.

for ethanol and benzene at high pressure are considerably higher than the prediction of equation (27). Satisfactory correlation of these results is obtained if the mean surface superheat at the critical condition, ΔT_0 in equation (27) has a value taken at the corresponding low pressure condition. Equation (27) applies only to clean, smooth, wetted surfaces. Results for clean, rough surfaces at low pressure appear to be correlated satisfactorily by equation (27) if the value of ΔT_0 is taken for the corresponding smooth surface condition.

The correlation is satisfactory for liquids as diverse as nitrogen and sodium. However, the points obtained from the nitrogen data are open to some doubt because of the wide divergence of the results obtained by two groups of experimenters [22], [23] and the uncertainty of the thermal conductivity estimation under conditions near to the critical [24].

ACKNOWLEDGEMENT

The author wishes to thank Mr. H. Hampson for many helpful discussions.

Table 1. Critical heat flux experimental data

Investigator	Reference	Symbol in Fig. 7	Substance	Surface material and condition	Surface geometry	Method of heating	Pressure lbf/in ²	ΔT , degf	\dot{q}_{bo} , critical heat flux, Btu/h ft ² $\times 10^{-3}$		
Noyes	7, 25	×	Sodium	Stainless steel, type 304	0.375 in dia. horizontal cylinder	Electrical, constant heat flux approach	0.58	27*	420		
							0.62	29*	480		
							0.96	31*	615		
			Molybdenum	0.375 in dia. horizontal cylinder	Electrical, constant heat flux approach	0.72	30*	500			
						1.10	31*	610			
						4.20	35*	780			
25	×	Sodium	Molybdenum	0.250 in dia. vertical cylinder	Electrical, constant pressure approach	1.70	70†	1,050			
						Stainless steel, type 304	0.250 in dia. vertical cylinder	Electrical, constant pressure approach	3.0	37‡	830
									14.7	73	78.5
Berenson	26	□	n Pentane	Copper, mirror finish	Horizontal flat plate	Steam	14.7	73	78.5		
							14.7	75	77		
Huber and Hoehne	27	◇	Benzene	Stainless steel, type 304	0.375 in. dia. horizontal cylinder	Electrical	13.5	43§	86		
							36.0	38§	107		
							51.0	32§	119		
							200.0	18§	154		
							300.0	14§	162		

	type 304	horizontal cylinder							
Braunlich	29	○	Water	Chrome plated copper	Tube	Steam	1.27	45	150
							2.22	45	175
							3.72	45	220
Akin and McAdams	30	●	Water	Nickel plated copper, polished	0.75 in dia. horizontal cylinder	Steam	6.00	45	243
							9.34	45	300
							14.70	45	390
Bonilla and Perry	31	△	Ethanol	Chrome plated copper	Horizontal flat disk	Electrical	14.70	65	155
Cichelli and Bonilla	32	▲	Ethanol	Chrome plated copper, repeatedly washed	Horizontal flat disk	Electrical	14.70	65	192
							375	27	350
							657	11	261
Akin and McAdams	30	▽	n Butanol	Nickel plated copper, polished	0.75 in dia. horizontal cylinder	Steam	14.7	60	105
Merte and Clark	22	⊕	Nitrogen	Copper	1 in dia. sphere	Transient cooling of sphere	14.7	25	45
Flynn, Draper and Roos	23	⊗	Nitrogen	Copper	0.625 in dia. horizontal cylinder	Electrical	14.7	18	18.5

Some values of thermal conductivity are obtained by extrapolation

- * Estimated from Fig. 6, reference 7.
- † Estimated from Fig. 21, reference 25.
- ‡ Estimated from Fig. 22, reference 25.
- § Estimated from Figs. 1 and 2, reference 27.
- || Estimated from Fig. 5, reference 32.

REFERENCES

1. Y. P. CHANG and N. W. SNYDER, Heat transfer in saturated boiling, *Chem. Engng Progr. Symp. Ser.* **56** (30) 25 (1960).
2. C. L. TIEN, A hydrodynamic model for nucleate pool boiling, *Int. J. Heat Mass Transfer* **5**, 533 (1962).
3. N. ZUBER, Nucleate boiling. The region of isolated bubbles and the similarity with natural convection, *Int. J. Heat Mass Transfer* **6**, 53 (1963).
4. J. N. ADDOMS, Heat transfer at high rates to water boiling outside cylinders, Sc.D. thesis, Chem. Eng., Mass. Inst. Tech. (1948); see also W. H. MCADAMS, *Heat Transmission*, Third Edition, p. 384. McGraw-Hill, New York (1954).
5. V. M. BORISHANSKY, An equation generalizing experimental data on the cessation of bubble boiling in a large volume of liquid, *Zhur. Tekh. Fiz.* **25**, 452 (1956). *Trans. Soviet Physics—Tech. Physics*, **1**, 438.
6. S. S. KUTATELADZE, A hydrodynamic theory of changes in the boiling process under free convection conditions, *Izv. Akad. Nauk SSSR, Otdel. Tekh. Nauk* No. 4, 529 (1951).
7. R. C. NOYES, An experimental study of sodium pool boiling heat transfer, AEC Rpt. *NAA-SR-6769* (1962); *J. Heat Transfer* **85**, 125 (1962).
8. R. G. DEISSLER, Columbia Univ. Heat Transfer Symp., New York (1954); see also [9].
9. R. COLE, A photographic study of pool boiling in the region of the critical heat flux, *J. Amer. Inst. Chem. Engrs* **6**, 533 (1960).
10. W. ROHSENOW and P. GRIFFITH, Correlation of maximum heat flux data for boiling of saturated liquids, *Chem. Engng Progr. Symp. Ser.* **52** (18) 47 (1956).
11. N. ZUBER, On the stability of boiling heat transfer, *Trans. Amer. Soc. Mech. Engrs* **80**, 711 (1958).
12. H. J. IVEY, Acceleration and the critical heat flux in pool boiling heat transfer, *Proc. Instn Mech. Engrs, Lond.* **177**, 15 (1963).
13. W. FRITZ, Berechnung des Maximalvolumens von Dampfblasen, *Phys. Z.* **36**, 379 (1935); quoted in M. JAKOB, *Heat Transfer*, Vol. 1, p. 630. John Wiley, New York (1959).
14. R. L. SEMERIA, An experimental study of the characteristics of vapour bubbles, *Symposium on Two Phase Flow*, p. 26. Inst. Mech. Engrs (1962).
15. A. S. PERKINS and J. W. WESTWATER, Measurements of bubbles formed in boiling methanol, *J. Amer. Inst. Chem. Engrs* **2**, 471 (1956).
16. R. F. GAERTNER and J. W. WESTWATER, Population of active sites in nucleate boiling heat transfer, *Chem. Engng Progr. Symp. Ser.* **56**, No. 30, 39 (1960).
17. L. E. SCRIVEN, On the dynamics of phase growth, *Chem. Engng Sci.* **10**, 1 (1959).
18. H. MERTE and J. A. CLARK, Pool boiling in an accelerating system, *J. Heat Transfer* **83**, 233 (1961).
19. R. W. GRAHAM and R. C. HENDRICKS, A study of the effect of multi-g accelerations on nucleate boiling ebullition, *NASA Tech. Note D-1196* (1963).
20. K. E. FORSTER and R. GREIF, Heat transfer to a boiling liquid, *J. Heat Transfer* **81**, 43 (1959).
21. F. C. GUNTHER and F. KREITH, Photographic study of bubble formation in heat transfer to subcooled water. Prog. Rpt. No. 4-120, Jet Propulsion Laboratory, Calif. Inst. Techn., 72 (1954).
22. H. MERTE and J. A. CLARK, Boiling heat transfer data for liquid nitrogen at standard and near zero gravity. *Advances in Cryogenic Engineering*, K. D. TIMMERHAUS, editor, Vol. 7, p. 546. Plenum Press, New York (1962).
23. T. M. FLYNN, J. W. DRAPER and J. J. ROOS, The nucleate and film boiling curve of liquid nitrogen at one atmosphere. *Advances in Cryogenic Engineering*, K. D. TIMMERHAUS, editor, Vol. 7, p. 539. Plenum Press, New York (1962).
24. H. ZIEBLAND and J. T. A. BURTON, The thermal conductivity of nitrogen and argon in the liquid and gaseous states, *Brit. J. Appl. Phys.* **9**, No. 2, 52 (1958).
25. R. C. NOYES, Boiling studies for sodium reactor safety, Part 1, AEC Rpt. *NAA-SR-7909* (1963).
26. P. J. BERENSON, Experiments on pool boiling heat transfer, *Int. J. Heat Mass Transfer*, **5**, 985 (1962).
27. D. A. HUBER and J. C. HOEHNE, Pool boiling of benzene, diphenyl and benzene-diphenyl mixtures under pressure, *J. Heat Transfer* **C85**, 215 (1963).
28. D. P. JORDAN and G. LEPPERT, Nucleate boiling characteristics of organic reactor coolants, *Nucl. Sci. Engng* **5**, 349 (1959).
29. W. H. MCADAMS, *Heat Transmission*, 3rd edn, p. 386. McGraw-Hill, New York (1954).
30. G. A. AKIN and W. H. MCADAMS, Boiling heat transfer in natural convection evaporators, *Trans. Amer. Inst. Chem. Engrs* **35**, 137 (1939); *Industr. Engng Chem.* **31**, 487 (1939).
31. C. F. BONILLA and C. W. PERRY, Heat transmission to boiling binary liquid mixtures, *Trans. Amer. Inst. Chem. Engrs* **37**, 685 (1941).
32. M. T. CICHELLI and C. F. BONILLA, Heat transfer to liquids boiling under pressure, *Trans. Amer. Inst. Chem. Engrs* **41**, 755 (1955).
33. D. T. JAMIESON and J. S. TUDHOPE, The thermal conductivity of liquids: a survey to 1963, D.S.I.R., Nat. Engng Lab. Rpt. No. 137 (1964).
34. J. TIMMERMANS, *Physico-chemical constants of pure organic compounds*. Elsevier, New York, (1950).
35. D. E. GRAY, editor, *American Institute of Physics Handbook*, 2nd edn. McGraw-Hill, New York (1963).
36. J. H. PERRY, editor, *Chemical Engineers' Handbook*, 4th edn. McGraw-Hill, New York (1963).
37. E. W. WASHBURN, editor, *International Critical Tables*. McGraw-Hill, New York (1933).

APPENDIX

The mean number of bubbles initiated in time δt per unit area of surface is:

$$\delta n_M = \dot{I}_M \delta t$$

At any instant, the mean volume of the bubbles which are initiated in time δt , are still attached,

and have existed for time t is:

$$\delta V = I_M V(t) \delta t$$

where

$$t < t_D$$

and $V(t)$ is the bubble volume. For non-coalescing spherical bubbles:

$$\delta V = I_M \cdot \frac{4\pi}{3} R(t)^3 \delta t$$

Hence the total volume of the attached bubbles per unit area of surface is:

$$l_M = \dot{I}_M \frac{4\pi}{3} \int_{t=0}^{t=t_D} R(t)^3 dt$$

$$= n_M R_D^3 \frac{4\pi}{3} \int_0^1 \frac{R}{R_D} \cdot d\left(\frac{t}{t_D}\right)$$

since

$$n_M = \dot{I}_M t_D$$

Hence $l = \phi n_M R_D^3$ where ϕ depends on the form of the bubble growth function for non-coalescing bubbles:

$$\phi = \frac{4\pi}{3} \int_0^1 \left(\frac{R}{R_D}\right)^3 \cdot d\left(\frac{t}{t_D}\right)$$

Résumé—Le concept de la similitude géométrique d'une distribution au hasard de bulles sphériques attachées à la surface d'ébullition est introduit et le mécanisme d'enlèvement des bulles à partir d'une surface plane horizontale dans l'ébullition nucléée saturée en réservoir est discutée. Le concept de la similitude géométrique est appliqué au régime de bulles en interaction dans l'ébullition nucléée en réservoir et ceci conduit à une expression pour le transport de chaleur à travers une sous-couche au repos que l'on suppose exister dans le fluide immédiatement au voisinage de la surface d'ébullition.

Le flux de chaleur dû à l'ébullition nucléée en réservoir est relié à la vitesse de production de vapeur à la surface d'ébullition. Le régime de bulles qui s'unissent dans l'ébullition nucléée en réservoir est étudié sur la base la similitude géométrique des frontières des phases. On suppose que le flux de chaleur critique a lieu pour une géométrie particulière du front des phases. Ceci conduit à la corrélation suivante pour le flux de chaleur critique dans l'ébullition saturée en réservoir pour des surfaces propres parfaitement mouillées:

$$q_{Bo} = 3,92 \cdot 10^{-4} [g\Delta T_0 K_L L^2 \rho_V (\rho_L - \rho_V)]^{0,333} \text{ en W/cm}^2$$

Cette expression corréle d'une façon satisfaisante les données du flux de chaleur critique pour une large gamme de liquides.

Zusammenfassung—Für Sieden im Sättigungszustand bei freier Konvektion wird geometrische Ähnlichkeit einer beliebigen Verteilung kugelförmiger Blasen an einer Siedefläche vorgeschlagen und der Blasenablösevorgang von der ebenen horizontalen Oberfläche für Sieden im Sättigungszustand bei freier Konvektion diskutiert. Die Vorstellung der geometrischen Ähnlichkeit wird auf das Gebiet sich gegenseitig beeinflussender Blasen beim Sieden in freier Konvektion angewandt und sie führt zu einem Ausdruck für den Wärmeübergang in einer ruhenden Unterschicht, die in der Flüssigkeit unmittelbar an der Siedefläche anliegend angenommen wird.

Die Wärmestromdichte beim Blasensieden wird zu der an der Heizfläche entstehenden Dampfmenge in Beziehung gesetzt. Auf Grund der geometrischen Ähnlichkeit der Phasengrenzen wird der Bereich der zusammenwachsenden Blasen beim Sieden in freier Konvektion untersucht. Es wird angenommen, dass die kritische Wärmestromdichte bei einer besonderen Geometrie der Phasenfront auftritt. Dies führt zu folgender Beziehung für die kritische Wärmestromdichte für Sieden im Sättigungszustand bei freier Konvektion an reinen, gleichmäßig benetzten Oberflächen:

$$q_{Bo} = 3,96 \times 10^7 [g\Delta T_0 K_L L^2 \rho_V (\rho_L - \rho_V)]^{1/3}$$

in Einheiten von W, s, m, kg

Dieser Ausdruck gibt eine zufriedenstellende Beziehung für Werte der kritischen Wärmestromdichte in einem weiten Bereich von Flüssigkeiten.

Аннотация—Вводится понятие геометрического подобия случайного распределения сферических пузырьков у поверхности нагрева, а также рассматривается механизм удаления пузырьков с горизонтальной плоской поверхности при пузырьковом кипении насыщенной жидкости в большом объеме. Понятие геометрического подобия применяется к режиму взаимодействия пузырьков при пузырьковом кипении, в результате чего получено выражение для теплообмена неподвижного подслоя, существование которого предполагается в непосредственной близости к поверхности нагрева.

Тепловой поток при пузырьковом кипении связан со скоростью парообразования на поверхности нагрева. Исследуется режим слияния пузырьков при пузырьковом кипении на основе геометрического подобия фазовых границ. Предполагается наличие критического теплового потока при кипении насыщенной жидкости в большом объеме для частного случая геометрии поверхности раздела. В результате получено следующее соотношение для критического теплового потока при кипении насыщенной жидкости в большом объеме для чистых гладких влажных поверхностей:

$$\dot{q}_{во} = 1,25 \{g\Delta T_0 K_L L^2 \rho_V (\rho_L - \rho_V)\}^{0,333} \text{ БТЕ/фут час}$$

Это выражение дает хорошую корреляцию данных о величине критического теплового потока для разнообразных жидкостей.